



HAL
open science

Extrema of micro-hardness in fully pearlitic compacted graphite cast iron

Jacques Lacaze, Charbel Moussa, Yannick Thebault, Wilson L Guesser

► **To cite this version:**

Jacques Lacaze, Charbel Moussa, Yannick Thebault, Wilson L Guesser. Extrema of micro-hardness in fully pearlitic compacted graphite cast iron. *International Journal of Cast Metals Research*, The, 2020, 33 (4-5), pp.218-225. 10.1080/13640461.2020.1832308 . hal-02966196

HAL Id: hal-02966196

<https://hal.science/hal-02966196>

Submitted on 13 Oct 2020

HAL is a multi-disciplinary open access archive for the deposit and dissemination of scientific research documents, whether they are published or not. The documents may come from teaching and research institutions in France or abroad, or from public or private research centers.

L'archive ouverte pluridisciplinaire **HAL**, est destinée au dépôt et à la diffusion de documents scientifiques de niveau recherche, publiés ou non, émanant des établissements d'enseignement et de recherche français ou étrangers, des laboratoires publics ou privés.

Extrema of micro-hardness in fully pearlitic compacted graphite cast iron.

J. Lacaze¹, C. Moussa², Y. Thébault¹, W.L. Guessser^{3†}

1 – CIRIMAT, université de Toulouse, ENSIACET, BP 44362, 31030 Toulouse, France

2 – MINES ParisTech, PSL – Research University, CEMEF – Centre de mise en forme de matériaux, CNRS UMR 7635, CS 10207, rue Claude Daunesse, 06904 Sophia Antipolis, France

3 - Tupy and UDESC, Rua Albano Schmidt, 3400 – 89227-901 - Joinville – SC - Brazil

Abstract

For improving mechanical strength of cast irons, a fully pearlitic matrix is sought by alloying with tin, copper and manganese. This applies in particular to the compacted graphite irons considered here. While average macro- and micro-hardness values were similar for the four fully pearlitic alloys under study, it was found that high copper and low tin content showed some very high maximum micro-hardness values, significantly higher than the corresponding mean. Such values may be seen as hard points in the material that would certainly impair machinability. Discussion of the reasons for these extreme values opens directions for further studies.

Keywords

Iron alloys, casting, carbon and graphite, hardness, pearlite

Corresponding author: J. Lacaze, jacques.lacaze@ensiacet.fr

Introduction

Use of compacted graphite cast iron (CGI) is strongly increasing nowadays as it shows better mechanical properties than lamellar graphite cast iron (LGI) and less micro-porosity than spheroidal graphite cast iron (SGI). CGI thus appears very well suited for further development of thin wall castings as required, in particular, in the automotive industry [1].

In order to have the highest possible mechanical properties, fully pearlitic CGIs are most often preferred. Such a matrix structure is obtained by alloying cast irons with copper, manganese and tin which are strong pearlite promoters. However, too high a level of any of these elements is known to be detrimental in one way or another, see e.g. Neumeier et al. [2]. Accordingly, optimizing the addition in pearlite promoter elements has long been of concern in the cases of SGI (see for example Yu et al. [3]) and LGI (see for example the review by Janowak and Gundlach [4]), but has received only little attention in the case of CGI [5]. In fact, the characteristics looked for pearlite are the same for all kinds of cast irons and were stated simply by Janowak and Gundlach: "fine pearlite with uniform strength and hardness". Such an aim calls for: 1) increasing pearlite fineness, i.e. decreasing the interlamellar spacing, which increases hardness and improves strength, and: 2) achieving a uniform interlamellar spacing of pearlite as it is thought to ensure uniform matrix hardness.

On the other hand, it is well known that cast irons with high hardness and fine interlamellar spacing of pearlite give rise to machinability difficulties. In a recent work dealing with drilling test of gray irons with different alloying elements, Silva [6] showed that tool life decreases as Brinell hardness and microhardness increase and proposed that this is a result of decreasing pearlite interlamellar spacing. This suggested further investigating the homogeneity of the material at the scale of the microstructure using micro-hardness measurements. In the present study, the effect of copper and tin in fully pearlitic CGI is considered at constant manganese content.

Experimental details

A series of nine melts were prepared in an induction furnace using a base melt having the composition listed in Table 1 to which various copper and tin additions were done in the treatment ladle. Chemical analysis was performed by Optical Emission Spectroscopy for all elements but sulfur and carbon which were measured by combustion. The control of the CGI liquid metal was carried out using the Sintercast Process with a special thermal analysis

procedure after the first addition of magnesium aimed at compacting graphite [7]. The final correction of magnesium content in the melts to reach 0.015 ± 0.004 wt.% and the inoculation treatment followed this thermal analysis. The melts were cast in stair castings with 7 stair thicknesses varying from 5 mm to 60 mm. The shake out time was 12 hours, meaning that all phase transformations happened with the part inside the mold.

Table 1 – Composition of the base melt (mass%).

C	Si	Mn	P	S	Cr	Ti	B	Sn	Cu
3.52	2.4	0.24	0.026	0.009	0.035	0.01	0.0001	0.018	0.183
Pb	Bi	Al	Mo	Sb	Ni	Nb	Zn	V	As
0.0003	0.0004	0.003	0.002	0.001	0.001	0.003	0.044	0.002	0.001

The stair 30 mm in thickness was selected for the present study and it was found that four of the nine melts showed a fully pearlitic matrix in the middle of the stair where all subsequent measurements were performed. The carbon, silicon, copper and tin contents of these four alloys are listed in Table 2. Figure 1 illustrates the microstructure of alloy B before (a) and after (b) Nital etching of the same area. For each alloy, three macro-hardness HB measurements have been performed with a load of 30 kg. On each sample, 100 micro-hardness HV measurements were carried out along a square grid having a 200 μm step size. Thanks to a slight etching of the metallographic sections, the exact location of each measurement could be adjusted by having each indent on one pearlite grain. Preliminary tests suggested using a charge of 100 g that leads to indent diagonals of 20-30 μm in length, corresponding to a maximum depth at the center of 3-4 μm . This depth is large enough to assume that etching did not affect the measurements.

Table 2 – Carbon, silicon, copper and tin contents (mass %) measured on the four selected samples, and macro-hardness values

Alloy reference	C	Si	Cu	Sn	HB
A	3.57	2.26	0.58	0.094	257
B	3.53	2.29	0.96	0.057	246
C	3.53	2.25	0.99	0.095	266
D	3.48	2.30	1.28	0.056	278

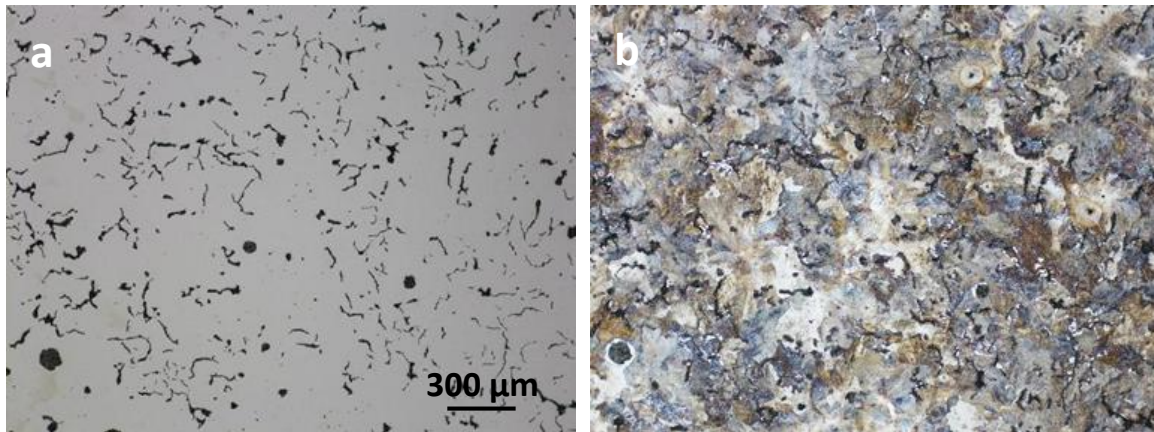


Figure 1 – Microstructure of alloy B before (a) and after (b) Nital etching. These micrographs represent the same area and the scale is the same for both.

Results and discussion

The average macro-hardness values listed in table 2 are in the expected range of values [3,4]. It is observed to increase slightly with Sn addition (compare alloys B and C) and with copper addition (compare alloys A and C or B and D).

Figure 2 shows an example of a micro-hardness indent which was properly located within a pearlite grain. Contrary to most observations during the present study, the interlamellar spacing was large enough to be resolved in this micrograph, certainly because of the inclination of the lamellae with respect to the metallographic section. Micro-hardness distributions appeared quite extended, which suggested representing them with percentiles as in figure 3. For each alloy, the average value is shown as a dot within a grey rectangle that contains 50% of the data while the upper and lower percentiles contain each 25% of the data. It is seen first that the average micro-hardness does very slightly increase with copper content as expected from literature [5] and in agreement with the slight increase in macro-hardness. However, the striking result is that the upper percentile enlarges dramatically when copper content increases and surprisingly when tin content decreases.

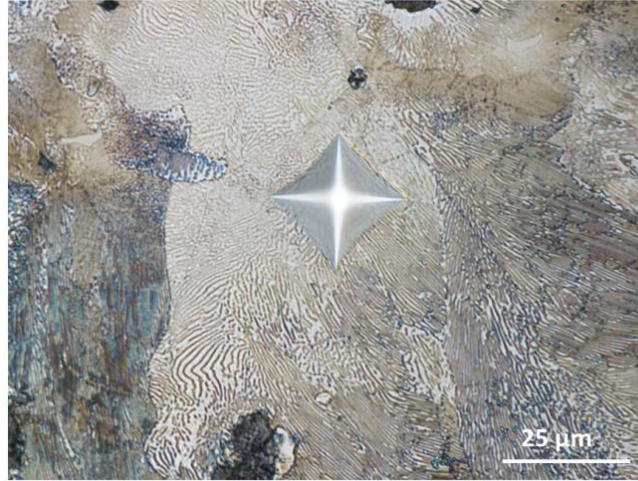


Figure 2 – Example of a micro-hardness indent within a pearlite grain where interlamellar spacing can be resolved (Alloy B).

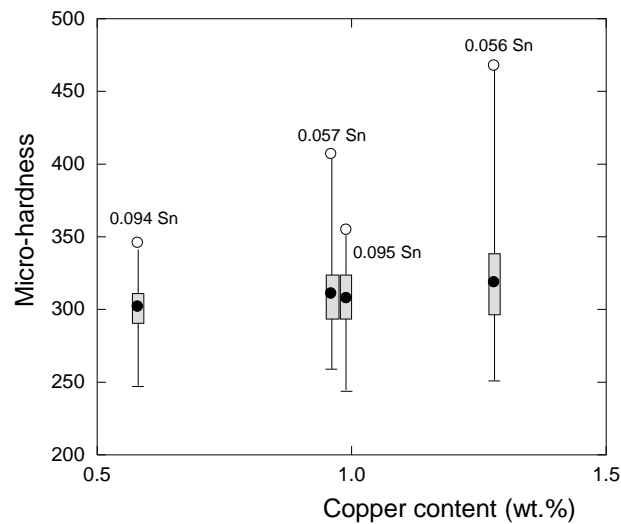


Figure 3 - Percentiles of pearlite micro-hardness distributions as a function of copper content.

The observed variability in the micro-hardness values is illustrated in Appendix A. To explain this result, it could first be argued that the variability of the micro-hardness values may be due to differences in the local internal stresses within the different pearlite grains. This possibility was checked by measuring the area of a few indents. Referring to Appendix B, it was concluded that micro-hardness variability is not caused by internal stress changes.

The mechanical response underneath a Vickers indenter is mainly defined by the material strength for a given representative strain which is strain hardening dependent [8].

Accordingly, the increase of the maximum micro-hardness values with copper content could

be thought to be due to an effect of interlamellar spacing because a smaller interlamellar spacing relates to a decreased average distance for dislocation motion as quantified by Ray and Mondal [9] for pearlitic steels. Therefore the interface density within the indented pearlite grains plays a major role in increasing the mechanical behavior and more precisely strain hardening. Copper decreases the interlamellar spacing of pearlite by about 10% in cast irons as reported by Svensson and Sjögren [10] and Nayyar et al. [11] who measured values changing from 300 to 100 nm when the cooling rate was increased from 0.005 to 1.9 °C/s. This effect of copper is small and could hardly explain the occurrence of high extrema as observed in the present work.

The most probable reason for explaining the effect of copper in cast irons appears to be the strong decrease in copper solubility with temperature in both austenite and ferrite and the associated potential precipitation of nearly pure copper (epsilon-Cu in the following). Figure 4 presents an isopleth Fe-Cu section that illustrates this decrease for a 3.5 wt.% carbon, 2.5 wt.% silicon and 0.24 wt.% manganese alloy. From this figure, such a precipitation is very much expected in ferrite of usual cast irons, even though they normally contain less than 1-1.5 wt.% copper. The associated strengthening mechanism has been characterized for Fe-Cu alloys [12] and has long found application to strengthen martensitic steels such as alloy 15-5 PH. A low temperature heat treatment of such an alloy leads to a nano-scale precipitation of epsilon-Cu in martensite between 673 K (400°C) and 773 K (500°C) as evidenced by differential thermal analysis [13].

Some work has been devoted to the study of this nano-precipitation of copper in steels and Fe-rich alloys by transmission electron microscopy (TEM). Chairuang Sri and Edmonds [14] have studied in detail the precipitation and ageing of epsilon-Cu in pearlite of alloys with about 1.5 wt.% carbon and 1.18 or 1.96 wt.% copper. Most of the precipitation occurs in the ferrite and at the interface between cementite and ferrite, but a small portion may also occur in the cementite constituent of pearlite. Murakami et al. [15] have studied the precipitation of epsilon-Cu during isothermal growth of pearlite in steels (0.8 wt.% carbon, 0.26 wt.% silicon and 0.35 wt.% manganese) alloyed with 0.06, 1.06 and 2.06 wt.% copper. In the case of the alloy with 2.06 wt.% Cu, they observed that epsilon-Cu precipitates both at the ferrite/austenite interface and in ferrite at 923 K (650°C), whereas it precipitates mainly in ferrite at 873 K (600°C). This precipitation results in an increase in the micro-hardness of the pearlite compared to that of the alloy with 0.06 wt.% Cu. In more recent studies, Razumakov

et al. [16] and Bataev et al. [17] have confirmed the effect of epsilon-Cu on hardening of ferrite and pearlite in standard steels and other low-silicon irons. They report a large increase in micro-hardness when the copper content varies up to 3.15 wt.%, followed by little change when the copper content is higher. Recent results by Gumienny et al. [5] show exactly the same evolution for compacted cast irons containing 1.0 to 3.8 wt.% copper.

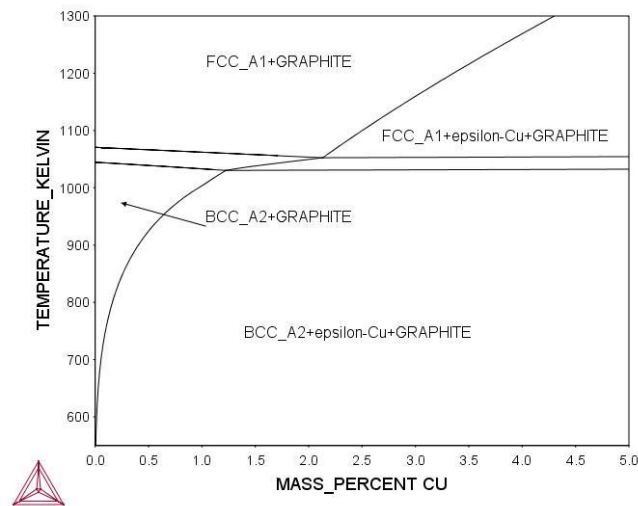


Figure 4 - Isopleth Fe-Cu section for an alloy containing 3.5 wt.% carbon, 2.4 wt.% silicon and 0.24 wt.% manganese. Calculation made with the THERMOCALC software and the TCFE-8 database. FCC_A1 and BCC_A2 stand respectively for austenite and ferrite.

Considering the evolution of micro-hardness during heat-treatment demonstrated by Murakami et al. [15], an attempt to use differential thermal analysis on the cast irons under study - as previously done for 15-5 PH alloy [13] - was carried out. This was not successful, probably because most of the copper precipitation was completed during cooling of the castings. It should be mentioned that the proof of copper precipitation in cast irons has already been made by Gilbert [18] in the case of alloys containing 0.5 to 1.0 wt.% copper. This was achieved by heat treatment of the alloys to make the precipitates coarser, which however leads to loss of information on the early stages of precipitation. Fortunately, although ferrite in conventional cast irons is magnetic at room temperature because of silicon, it has recently been shown that imaging of copper precipitates by TEM is possible [19]. This opens up possibilities for investigating and optimizing early stages of copper precipitation.

Finally, the most unexpected and still unexplained result is the effect of tin addition which decreases the maximum pearlite micro-hardness values. In fact, when the tin content is

increased, the macro-hardness increases, the average micro-hardness almost does not change and the micro-hardness maximum value decreases. This latter decrease is thus probably due to a local phenomenon. It is hypothesized that it is related to tin decreasing the undercooling for pearlite nucleation thanks to precipitation of a transient Fe_3SnC phase at the graphite/matrix boundary [20]. This would lead to an increase in the interlamellar spacing for given casting conditions and cooling rate and thus to a decrease in micro-hardness close to graphite precipitates. Note that this explanation would apply to fully pearlitic matrix and not to cast irons containing some ferrite located around graphite precipitates as in the recent work by Lyu et al. [21]. This suggestion would be worth dedicated experiments involving isothermal growth of pearlite after austenitization.

Conclusion

Fully pearlitic compacted graphite cast irons alloyed with high copper and low tin contents showed maximum micro-hardness values which are significantly higher than for pearlite in alloys with low copper and tin contents. It was further observed that high values of tin decrease these maximum values. The effect of high copper content in increasing micro-hardness values may be convincingly related to precipitation of epsilon-Cu while the effect of high tin content is suggested to relate to coarser pearlite. In practice, precipitation of epsilon-Cu leading to hard points in the matrix may be detrimental to machining performances and the present results suggest limiting copper additions to 1 % mass in fully pearlitic cast irons.

Acknowledgment

Thanks are due to David de Jonghe for performing the micro-hardness measurements during a one month internship at CIRIMAT laboratory. This research did not receive any specific grant from funding agency in the public, commercial, or not-for-profit sectors.

References

- [1] S. Dawson, W.L. Guesser, Castability, product design, and production of compacted graphite irons, in D.M. Stefanescu (Ed.), ASM Handbook, Vol. 1A, Cast Iron Science and Technology, ASM International, Materials park, 2017, pp. 665.
- [2] L.A. Neumeier, B.A. Betts, D.H. Desy, Tin and copper combinations in as-cast ductile iron, AFS Trans. 82 (1974) 131.

- [3] S.K. Yu, C.R. Loper, H.H. Cornell, The effect of molybdenum, copper, and nickel on the microstructure, hardness, and hardenability of ductile cast irons, *AFS Trans.* 94 (1986) 557.
- [4] J.F. Janowak, R.B. Gundlach, A modern approach to alloying gray iron, *AFS Trans.* 90 (1982) 847.
- [5] G. Gumienny, B. Kacprzyk, J. Gawroński, Effect of copper on the crystallization process, microstructure and selected properties of CGI, *Archives of Foundry Engineering* 17 (2017) 51-56
- [6] A.E. Silva, Furação de ferros fundidos de alta resistência aplicados em cabeçotes de motores. Master Thesis, Federal University of Uberlândia, Brazil, 2016.
- [7] W. Guesser, T. Schroeder, S. Dawson, Production experience with compacted graphite iron automotive components, *AFS Trans.* 109 (2001) 63.
- [8] X. Hernot, C. Moussa, O. Bartier, Study of the concept of representative strain and constraint factor introduced by Vickers indentation, *Mechanics of Materials* 68 (2014) 1-14
- [9] K.K. Ray, D. Mondal, The effect of interlamellar spacing on strength of pearlite in annealed eutectoid and hypoeutectoid plain carbon steels, *Acta Metal. Mater.* 39 (1991) 2201-2208
- [10] H. Svensson, T. Sjögren, The effect of cooling rate, section size and alloying on matrix structure formation in pearlitic grey cast iron, *Key Engineering Materials* 457 (2011) 169-174
- [11] V. Nayyar, H. Svensson, M. König, A. Berglund, L. Nyborg, Investigation of microstructure and material properties of 18 different graphitic cast iron model materials with focus on compacted graphite iron (CGI), *Int. J. Microstructure and Materials Properties* 8 (2013) 262-282
- [12] K. Nakashima, Y. Futamura, T. Tsuchiyama, S. Takaki, Interaction between dislocation and copper particles in Fe-Cu alloys, *ISIJ Int.* 42 (2002) 1541-1545
- [13] E. Herny, E. Andrieu, J. Lacaze, F. Danoix, N. Lecoq, Study by differential thermal analysis of reverse spinodal transformation in 15-5 PH alloy, *Solid State Phenomena* 172-174 (2011) 338.
- [14] T. Chairuangsi, D.V. Edmonds, The precipitation of copper in abnormal ferrite and pearlite in hyper-eutectoid steels, *Acta mater.* 48 (2000) 3931-3949
- [15] M. Murakami, Y. Takanaga, N. Nakada, T. Tsuchiyama, S. Takaki, Microstructure and mechanical property of copper bearing eutectoid steel, *ISIJ Int.* 48 (2008) 1467-1472
- [16] A.A. Razumakov, N.V. Stepanova, I.A. Bataev, O.G. Lenivstseva, I.I. Riapolova, K.I. Emurlaev, The structure and properties of cast iron alloyed with copper, *IOP Conf. Series, Mater. Sci. Eng.* 124 (2016) 012136.

- [17] I.A. Bataev, N.V. Stepanova, A.A. Bataev, A.A. Razumakov, Ferrite and perlite hardening in copper-alloyed steels and irons, *Russian Physics J.* 60 (2017) 1017-1021
- [18] G.N.J. Gilbert, Properties of pearlitic and annealed ferritic nodular-irons alloyed with copper, *Foundry Trade J.* 121 (1966) 507.
- [19] L.N. Garcia, A.J. Tolley, F.D. Carazo, R.E. Boeri, Identification of Cu-rich precipitates in pearlitic spheroidal graphite cast irons, *Mater. Sci. Tech.*, 35 (2019) 2252-2258
- [20] J. Lacaze, J. Sertucha, Effect of tin on the phase transformation of cast irons, *J. Phase Equi. Diff.* 38 (2017) 743.
- [21] Y. Lyu, Y. Sun, S. Liu, J. Zhao, Effect of tin on microstructure and mechanical properties of compacted graphite iron, *Int. J. Cast Met. Res.* 28 (2015) 263-268
- [22] A. Freulon, J. Sertucha, J. Lacaze, Solidification and room temperature microstructure of a fully pearlitic compacted graphite cast iron, *Transactions of the Indian Institute of Metals*, 71 (2018) 2651-2656
- [23] T.Y. Tsui, W.C. Oliver, G.M. Pharr, Influences of stress on the measurement of mechanical properties using nanoindentation: Part I. Experimental studies in an aluminum alloy, *Journal of Materials Research*, 11 (1996) 752-759

Appendix A

It is seen in figure 3 that the minimum micro-hardness values of the pearlite are nearly the same for all alloys. A micrograph of most of the corresponding largest indents was taken as illustrated in figure A1 for alloys B and C. In some cases, it was seen that the indent may have been affected by a nearby graphite particle as in figure A1-b, thus explaining the lower hardness value. However, this does not seem to be verified in most cases, e.g. the indent in figure A1-a where the large interlamellar spacing seen on this section plane could instead be the explanation.

Figure A2 presents similarly indents for highest micro-hardness values for the same alloys as in figure A1. While most of these small indents were made in grains containing pearlite too fine to be resolved by optical microscopy (e.g. figure A2-b), this is not the case of the one in figure A2-a. Thus, it seems there is no one to one relation between the lamellar spacing seen on the section plane and the micro-hardness value, and this has been seen described quantitatively elsewhere [22].

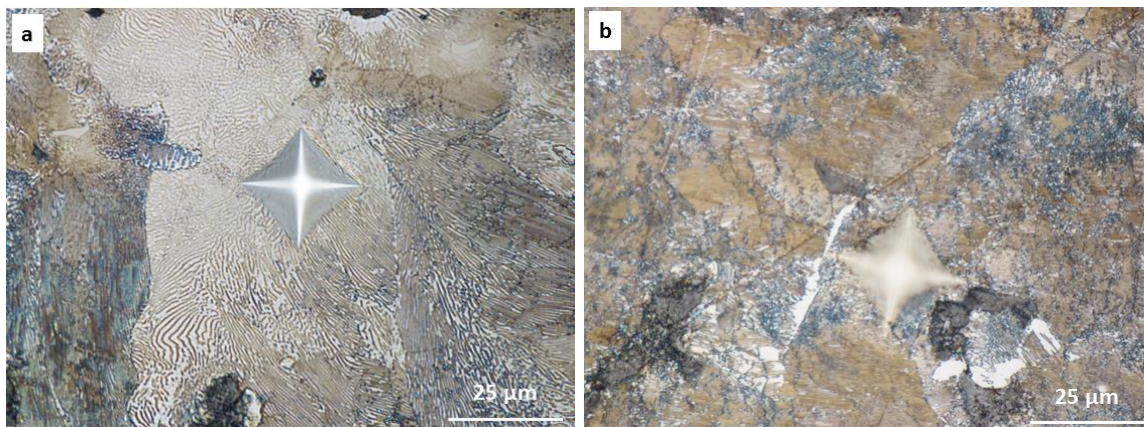


Figure A1: micro-hardness prints with low micro-hardness value for alloys B (a) and C (b).

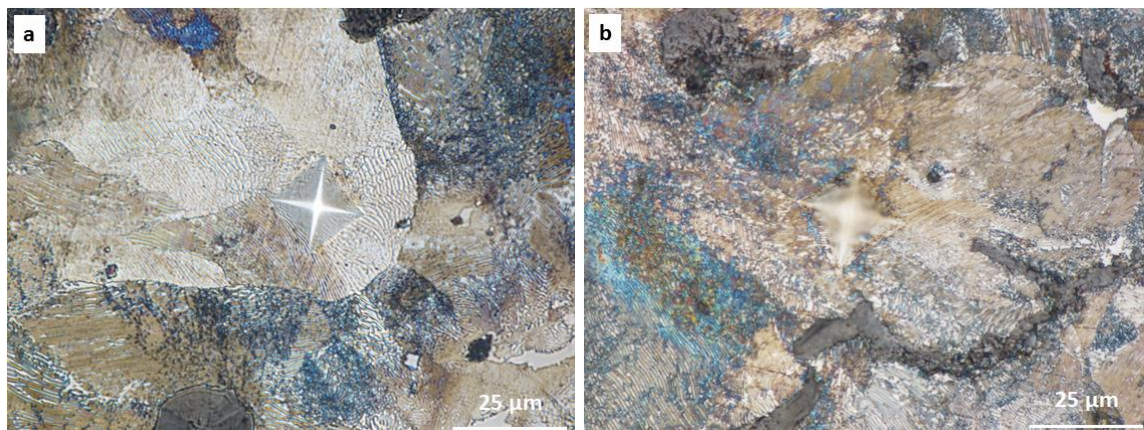


Figure A2: micro-hardness prints with high micro-hardness value for alloys B (a) and C (b).

One further example illustrating the possible variation in micro-hardness is seen in figure A3 where two indents associated to highly different micro-hardness values were performed. These indents have been observed also by scanning electron microscopy (SEM) as shown in figure A4. It is clearly seen that the large indent (figure A4-a) corresponding to the smaller micro-hardness value has led to a crack initiated at a grain boundary and to delamination of the lamellas. On the contrary, the small indent (figure A4-b) does not present apparent mechanically induced defects other than a plastic deformation of the lamellas.



Figure A3: micro-hardness prints in two pearlite grains showing close lamellar spacing (alloy B).

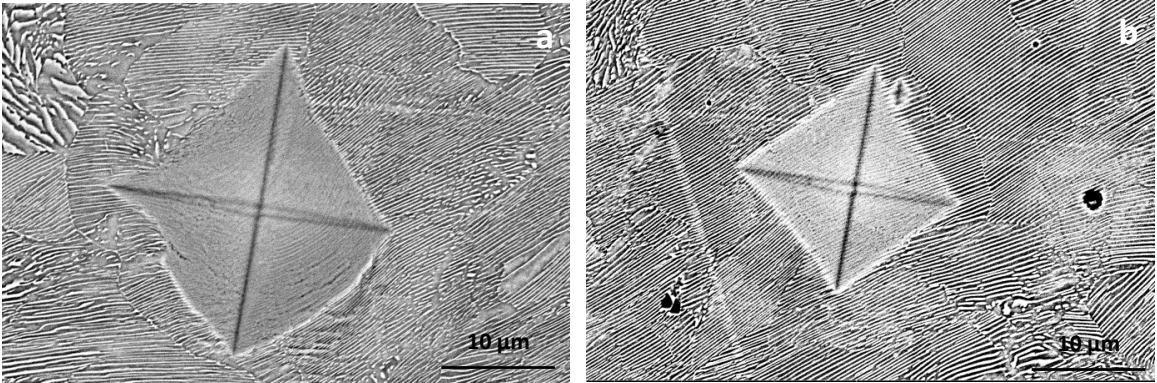


Figure A4: SEM micrograph of each of the micro-hardness prints seen in figure A3.

Appendix B

The influence of internal stresses on the measurement of Berkovich hardness was studied by Tsui et al. [23]. In fact, internal stresses influence displacement depth of the indenter within the material and also the shape of the indent with more or less pile-up or sink-in, whatever the indenter shape. Compressive internal stresses tend to increase the pile-up or decrease the sink-in of the imprint while tension internal stresses act in the opposite way. The influence of internal stresses on the indenter displacement is thus compensated by the pile-up or sink-in of the imprint while the contact surface (or the projected area) between the indenter and the material is not influenced. However, Vickers hardness is generally calculated using the diagonals length which relies on the assumption that the indent presents no pile-up or sink-in. A schematic is presented in Figure B1 to illustrate the errors on hardness measurement that can be made due to internal stresses. When no internal stresses are present, figure B1-a, there is no pile-up or sink-in. If compressive or tension internal stresses are present the imprint presents pile-up (figure B1-b) or sink-in (figure B1-c), respectively. The 3 cases of figure B1 have different diagonals, therefore they will have different hardness values when evaluated using the diagonals. However, the projected areas defined with the dashed lines are equal for the 3 cases. Therefore, using the projected area to calculate the hardness will lead to the same value for the 3 cases, which is correct since internal stresses should not influence the hardness value of the material as this is an intrinsic property.

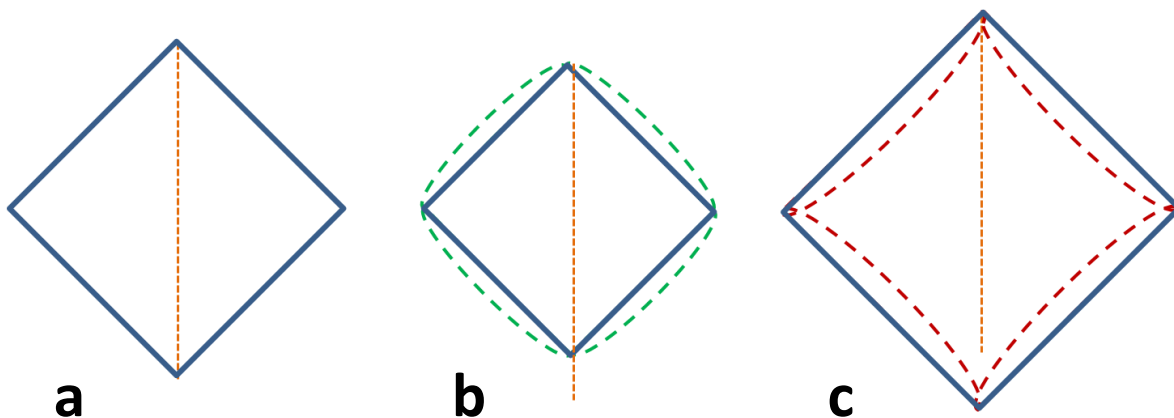


Figure B1. Schematic illustration of the influence of internal stresses on the diagonal length and on the projected area of Vickers indents. (a) no internal stresses leading to no pile-up or sink-in, (b) compressive internal stresses leading to an increase of pile-up, (c) tension internal stresses leading to an increase of sink-in. The 3 cases have the same projected area indicating the same hardness.

To verify if the variability observed in the micro-hardness values during the present study could be due to internal stresses variability, micro-hardness was calculated using the diagonals and the projected area. Two indents giving different hardness values were analyzed. The micro-hardness was evaluated using diagonals, on the one hand, and the projected area, on the other hand, see figure B2. Both calculation methods gave similar results which indicate that the micro-hardness variability is not due to local internal stresses.

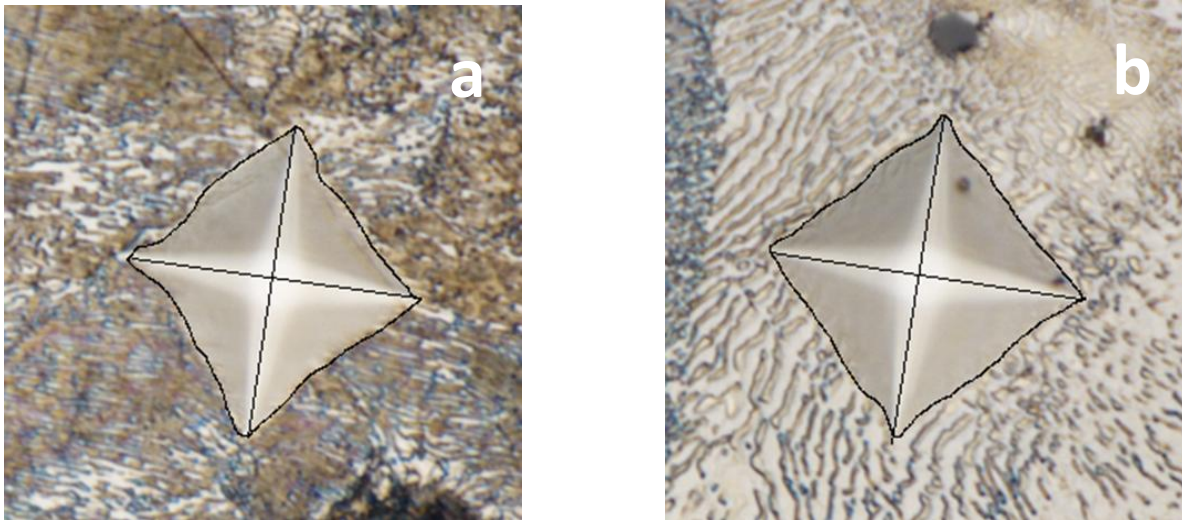


Figure B2. Two micro-hardness indents with HV=352 (a) and HV=293 (b). Solid lines indicate the diagonals and delimit the projected area used for hardness calculations..